

Processability and Mechanical Properties for Binary Blends of PP and LLDPE Produced by Metallocene Catalyst

Kazuya Ono,^{1,2} Hiroaki Ogita,² Kenzo Okamoto,¹ Masayuki Yamaguchi¹

¹*School of Materials Science, Japan Advanced Institute of Science and Technology, Nomi, Ishikawa 923-1292, Japan*

²*Nihon Tetra Pak K. K., 755-1 Jinba-Uenohara, Gotemba, Shizuoka 412-0047, Japan*

Received 18 September 2008; accepted 21 December 2008

DOI 10.1002/app.29922

Published online 8 May 2009 in Wiley InterScience (www.interscience.wiley.com).

ABSTRACT: Processability at extrusion coating and mechanical properties of the films obtained are investigated by means of linear and nonlinear rheological measurements and tensile tests for blends of polypropylene (PP) and linear low-density polyethylene (LLDPE). Both materials are produced by metallocene catalyst. The processability of PP is found to be improved by the addition of LLDPE; the blend shows low level of motor torque and head pressure in an extruder and small level of neck-in as compared with pure PP.

Further, the anisotropy of ultimate tensile strength, which is prominent for PP, is reduced by blending with LLDPE. As a result, the blend having 20 wt % of LLDPE shows appropriate properties in the molten state for extrusion coating and in the solid state as a film. © 2009 Wiley Periodicals, Inc. *J Appl Polym Sci* 113: 3368–3375, 2009

Key words: polypropylene; polyethylene; extrusion; rheology; blends

INTRODUCTION

It is well known that a low-density polyethylene (PE) produced by the radical polymerization method at high temperature and pressure is widely used for extrusion coating because of the excellent processability originating from the long-chain branch structure.^{1,2} For example, the marked non-Newtonian behavior in shear viscosity, which is attributed to the broad distribution of relaxation time because of broad molecular weight distribution as well as the existence of long-chain branches, leads to low level of motor torque at a high output condition. Furthermore, the strain hardening in transient elongational viscosity is responsible for a small level of neck-in, defined as the lateral reduction of the extruded film. The origin of the strain-hardening for a branched polymer has been well explained by chain stretching between branch points.^{3–7} In contrast, the rheological properties of isotactic polypropylene (PP) are not suitable for extrusion coating owing to the essentially linear molecular structure. In particular, no or weak strain-hardening in elongational viscosity is responsible for large neck-in and draw resonance.^{8,9} However, various attractive properties of PP, such as stiffness, heat resistance, grease proofness, and stress cracking resistance, are desired for packaging of food and beverage;^{2,10} a large part of them are

produced by extrusion coating. Therefore, intensive efforts have been made to enhance the elastic nature of PP even at high temperature, because extrusion coating is performed at high temperature to oxidize the polymer for good adhesion with substrate.

One of the most conventional approaches to modifying rheological properties is the incorporation of long-chain branches.^{11–15} Although branched PP shows marked strain-hardening in elongational viscosity, the obtained products sometime have a problem with odor. This is ascribed to volatile components generated by the thermal degradation of chemical compounds added in order to incorporate the long-chain branches. Moreover, mixing with a small amount of critical gel is known to be a significantly effective way to enhance strain-hardening behavior.¹⁶ The critical gel is defined as a weak gel which is just beyond the critical point of sol–gel transition. However, the thermal degradation of the critical gel also leads to odor and off-taste, which prohibit the blend from being applied in food packaging.¹⁷ Polymer blend technique is also employed to modify rheological properties, especially for miscible blends.¹⁸ In case of immiscible blends, however, blending another polymer has scarce impact on the strain-hardening behavior in elongational viscosity because the density of entanglement couplings in a continuous phase is unchanged.¹⁸

It has been generally accepted that PP is immiscible with PE, and their blend shows phase-separated morphology.^{19,20} However, recent study has revealed that a linear low-density polyethylene with a large

Correspondence to: M. Yamaguchi (m_yama@jaist.ac.jp).

amount of short-chain branches which is produced by metallocene catalyst shows low interfacial tension with PP, leading to interfacial thickness.^{21,22} McNally et al.²³ showed that an ethylene-1-octene copolymer having 25 wt % of 1-octene is partially miscible with PP when the copolymer content in the blend is less than 10 wt %. The interfacial tension between PP and ethylene- α -olefin copolymers was evaluated by Carriere and Silvis.²⁴ They found that interfacial tension decreases with increasing α -olefin content. Moreover, low interfacial tension between PP and ethylene-1-hexene copolymer was detected by Yamaguchi and Miyata²² using a rheological emulsion model. They also found that ethylene-1-butene and ethylene-1-hexene copolymers having more than 50 mol % of α -olefin are thermodynamically miscible with PP in a molten state.^{20,21} Furthermore, Razavi-Nouri²⁵ clarified that copolymerization of ethylene into a polypropylene improves the compatibility with ethylene- α -olefin copolymers synthesized by metallocene catalyst. Finally, Chaffin et al.²⁶ studied heat-seal strength of PP and PE, and found that good seal strength is obtained for laminated sheets when both PE and PP are produced by metallocene catalyst.

In this study, commercially available metallocene linear low-density polyethylene, which is designed for extrusion coating, is employed to improve the extrusion processability of PP with a small amount of ethylene. Further, the miscibility, rheological properties, processability, and mechanical properties of the film extruded by a T-die are investigated.

EXPERIMENTAL

Materials and processing

Commercially available isotactic polypropylene (PP) containing a small amount of ethylene unit as a comonomer, which is produced by metallocene catalyst, was employed in this study. The melt flow rate (MFR) is 7 g/10 min at 230°C and the density is 898 kg/m³. Furthermore, a linear low-density polyethylene (LLDPE), which is also commercially available as extrusion coating grade, was used. The MFR is 13 g/10 min at 190°C and the density is 913 kg/m³.

Similar to a conventional processing machine and conditions, a single-screw extruder (Toyoseiki, Laboplastmill, Tokyo, Japan), which is good enough for mixing at actual processing, equipped with a T-die was used for the film extrusion. The diameter of the screw was 20 mm and L/D ratio was 24. The width of the T-die was 150 mm and the screw rotation speed was 40 rpm. Prior to feeding the samples into the hopper, two resins in a pellet form were manually mixed. The blend ratios of PP and LLDPE are 100/0, 90/10, 80/20, 50/50, and 0/100 (PP/LLDPE) by weight. The motor torque, head pressure, output

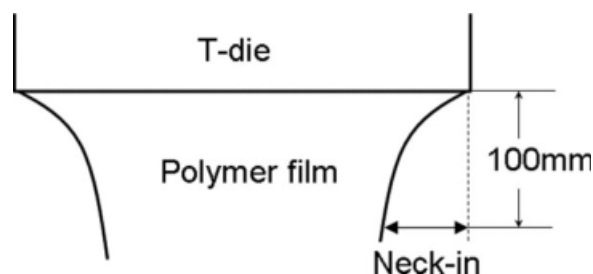


Figure 1 Definition of neck-in at extrusion-coating.

rate, and neck in level were measured at 260°C. The neck in was defined as the lateral reduction of the width of a free-falling molten film. In this study, the reduction at 100 mm under the die was measured as illustrated in Figure 1.

The blend samples were also prepared by melt mixing in a 50 cm³ internal batch-type mixer (Toyoseiki, Laboplastmill, Tokyo, Japan) at 145°C for 20 min. In order to measure the rheological properties at an equilibrium condition, that is, without thermal degradation, thermal stabilizers such as a hindered phenol (Ciba, Irganox 1010) and a phosphate (Ciba, Irgafos 168) were added. The amount of each stabilizer was 0.05%. The obtained samples were compressed into flat sheets at 160°C by a laboratory compression molding machine.

Measurements

Thermal analysis was conducted by a differential scanning calorimeter (Mettler-Toledo, DSC 820, Tokyo, Japan) using a sample of about 3 mg under a nitrogen atmosphere to avoid degradation. After cooling from 190°C to 30°C at a rate of 10°C/min, the melting profile was recorded at a heating rate of 10°C/min.

The frequency dependence of the oscillatory shear moduli in the molten state was measured by a cone and plate rheometer (UBM, MR500, Muko, Japan) at various temperatures. Measurements were carried out in a linear region under a nitrogen atmosphere. The diameter of the cone was 25 mm, and the angular frequency range was from 0.1 to 120 s⁻¹.

Steady-state shear viscosity was evaluated by a capillary rheometer (Capillograph, Toyoseiki, Tokyo, Japan) with a circular die having the following dimensions: π of the entrance angle, 1 mm in diameter, and 20 mm in length. The resin temperature in the cylinder and the die was kept at 190°C.

The drawdown force, defined as the force needed for the extension of a polymer extrudate, was evaluated by the capillary rheometer with a circular die having the following dimension; $\pi/2$ of the entrance angle, 2.095 mm in diameter, and 8 mm in length. The resin temperature in the cylinder and the die was kept at 160°C, and the draw ratio was 7.5.

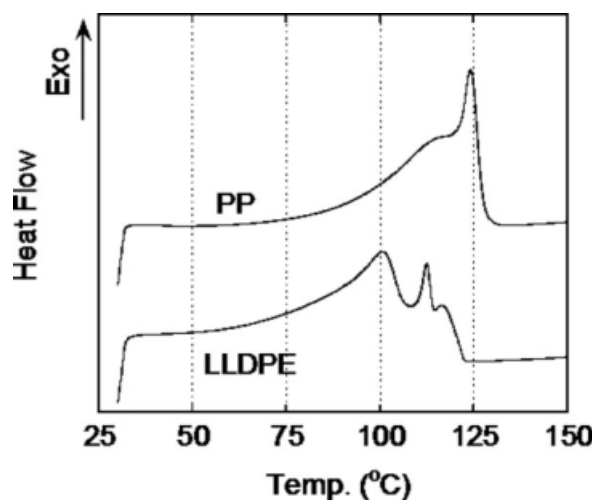


Figure 2 DSC heating curves of PP and LLDPE employed in this study. The heating rate is 10°C/min.

The dynamic mechanical properties as a function of temperature were measured by a dynamic mechanical analyzer (UBM, DVE E4000, Muko, Japan) at 10 Hz. The rectangular specimen was cut out from the compression-molded plaque. The heating rate was 2°C/min.

Tensile test of the films was carried out using a tensile tester (Autograph AG-1, Shimadzu, Kyoto, Japan) at room temperature. The stress was determined from dividing the tensile load by the initial cross-sectional area, and the strain was calculated from the ratio of the increment of the length between clamps to the initial gauge length. In this study, two samples were prepared in order to examine the mechanical anisotropy; the MD sample was cut out from the film parallel to the flow direction, and the TD sample was cut perpendicular to the flow direction. In the case of the MD sample, therefore, the direction of the tensile deformation coincided with the flow direction. The measurements were performed five times for each sample, and the average value was calculated.

RESULTS AND DISCUSSION

Characterization of polymers

Prior to the evaluation of the blend samples, the thermal and rheological properties of the PP and LLDPE employed in this study were investigated. Figure 2 shows DSC heating curves of PP and LLDPE. As seen in the figure, the melting point of PP is about 124°C, which is significantly lower than that of a conventional propylene homopolymer—165°C. Further, PP shows a single peak in the heating curve, which is fairly different from a conventional propylene-ethylene random copolymer produced by Ziegler-Natta catalyst. Uniform distribution of the ethylene unit is responsible for the thermal property. In contrast, double peaks are

clearly detected in LLDPE at 112 and 100°C. Furthermore, a weak shoulder peak is observed at 116°C. The result demonstrates that the LLDPE employed in this study is a blend sample. Considering the processability and rheological properties in a molten state, which suggest that the molecular weight and its distribution are typical for an extrusion coating grade, as shown later, the peak located at 112°C is attributed to the melting point of a low-density polyethylene and the one at 100°C is attributed to a linear low-density polyethylene produced by metallocene catalyst. Although the blend ratio and the content of comonomer in the LLDPE are unknown, the DSC profile indicates that the LLDPE is the major component. Furthermore, the comonomer content is crudely predicted by the melting point as compared with the findings of previous studies summarized in Table I,^{27–31} although it should be noted that the melting point of the LLDPE is enhanced to some extent by the addition of another PE showing a higher melting point.²⁹ Moreover, the comonomer content is also predictable from the density data.^{28,31,32}

The master curves of the oscillatory shear moduli for PP and LLDPE are shown in Figure 3. The reference temperature is 190°C. The apparent flow activation energy is calculated from the slope of the logarithm of the shift factor plotted against the reciprocal of absolute temperature (Arrhenius plot), following the well-known Andrade equation.³³ The flow activation energy is found to be 37.3 kJ/mol for PP and 37.7 kJ/mol for LLDPE. The value of PP is slightly lower than that of a conventional propylene homopolymer. In contrast, LLDPE shows large activation energy as compared with a conventional LLDPE. A large amount of α -olefin unit as well as the mixing of a low-density PE is responsible for the high activation energy, although the species of α -olefin hardly affects the activation energy. In case of an LLDPE, it is known that the flow activation energy ΔH increases with short-chain branches as follows:³⁴

$$\Delta H = 23.9 + 26.8 \left[1 - \exp \left(- \frac{\text{SCB}/1000\text{CH}_2}{35.4} \right) \right]. \quad (1)$$

Suppose that number of short-chain branches (SCB/1000CH₂) of the LLDPE is 18.5 per 1000 carbon atoms

TABLE I
 T_m and Comonomer Content in Linear Low-Density Polyethylene

Polymer	Comonomer content (mol %)	T_m (°C)	Reference
Ethylene- α -olefin	2.2–2.5	100	27
Ethylene-1-butene	5.0	98.7	28
Ethylene-1-hexene	3.7	97	29
Ethylene-1-octene	5.0	98	30
Ethylene-1-decene	3.7	100	31

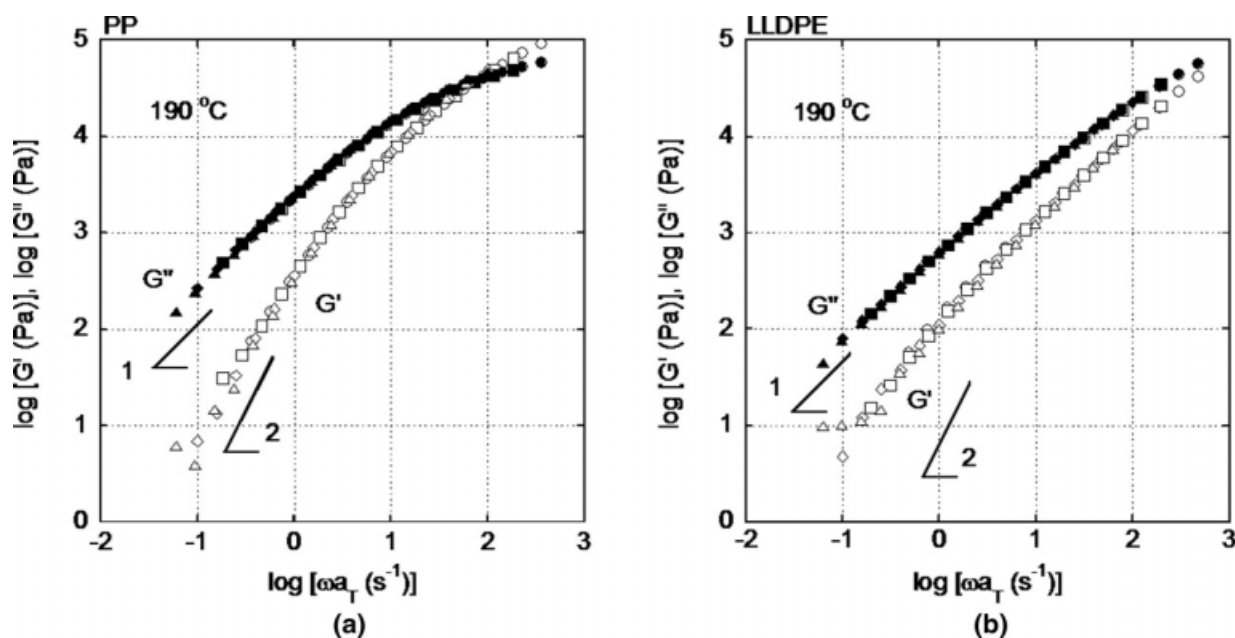


Figure 3 Master curves of frequency dependence of oscillatory shear moduli for (a) PP and (b) LLDPE employed in this study. The reference temperature is 190°C.

(3.7 mol % of α -olefin), the activation energy is 34.8 kJ/mol, which is slightly lower than the experimental value. Therefore, there would be a contribution of the low-density polyethylene to some degree.

Although the time-temperature superposition principle seems to be applicable to both polymers, detailed characterization by Van Gorp-Palmen plot³⁵ reveals that LLDPE shows thermorheological complexity (the data obtained at different temperatures

are not superposed perfectly), as seen in Figure 4. The results demonstrate that the molecular aggregation state in LLDPE is dependent on the temperature. The same result was reported on binary blends composed of an LLDPE by Ziegler-Natta catalyst and a low-density polyethylene.³⁶ As seen in Figure 3, the relatively high level of storage modulus in the low frequency region for LLDPE is also attributed to the blending of a low-density polyethylene. It is

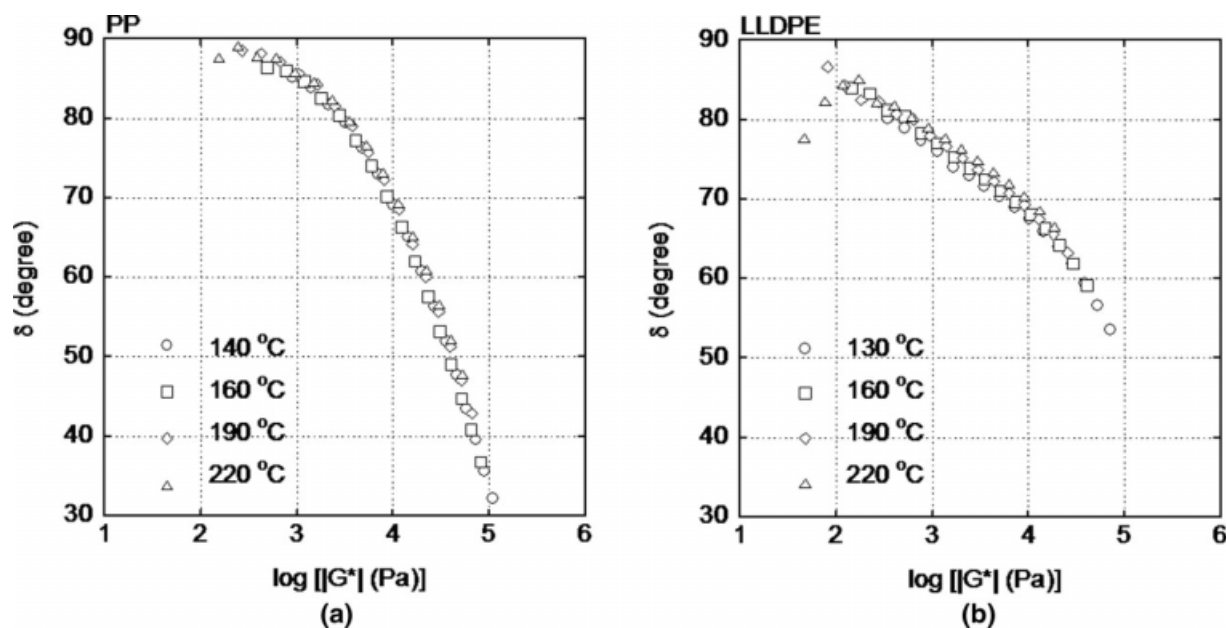


Figure 4 Van Gorp-Palmen plots for (a) PP and (b) LLDPE at various temperatures.

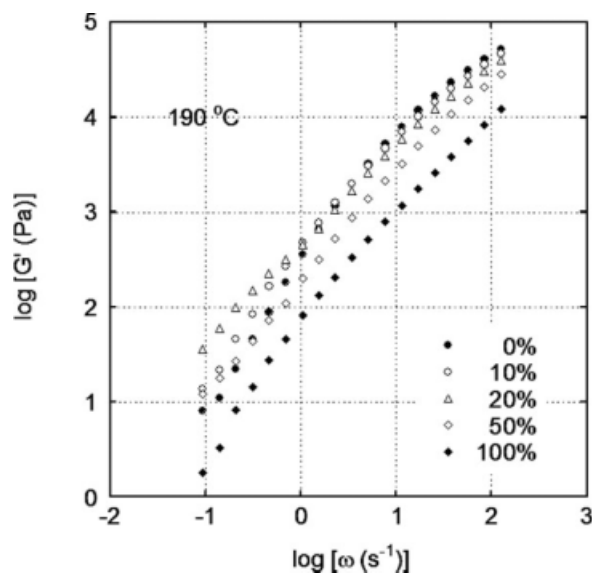


Figure 5 Frequency dependence of shear storage modulus G' at 190°C for PP, LLDPE, and the blends. The numbers in the figure represent the content of LLDPE.

generally accepted that a low-density polyethylene has a broad relaxation time, leading to high G' in the low frequency region.

The thermal and rheological characterization reveals that the LLDPE employed in this study is a blend of an LLDPE produced by metallocene catalyst and a conventional low-density polyethylene.

Rheological properties

Figure 5 shows the shear storage modulus G' for all the samples at 190°C plotted against the angular fre-

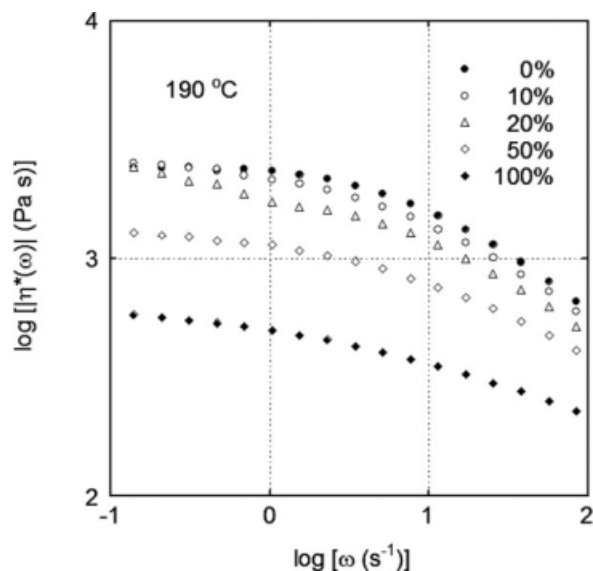


Figure 6 Absolute value of complex shear viscosity $|\eta^*(\omega)|$ at 190°C for PP, LLDPE, and the blends. The numbers in the figure represent the content of LLDPE.

quency. In the high frequency region, PP shows the highest G' , whereas LLDPE shows the lowest. In the low frequency region, however, PP/LLDPE (80/20) blend exhibits the highest G' . This could be attributed to the relaxation of the deformed droplets by interfacial tension,^{16,37,38} demonstrating that the blend is an immiscible system.

The absolute value of complex shear viscosity $|\eta^*(\omega)|$ at 190°C was plotted against the angular frequency in Figure 6. Although the Cox–Merz empirical rule is not applicable to heterogeneous melts, the figure suggests the order of the shear viscosity in the extruder. In the high frequency region, which gives important information on the head pressure at conventional processing condition, the complex viscosity decreases with increasing LLDPE content.

The steady-state shear viscosity at the high shear rate region was evaluated by a capillary rheometer at 190°C as shown in Figure 7. As seen in the figure, shear viscosity of PP at the high shear rate region (beyond 10s^{-1}) is lower than that of LLDPE. This is attributed to the pronounced shear thinning behavior of PP. Furthermore, the shear viscosities of the blends are almost similar to those of PP at the high shear rate region.

The drawdown force was also measured to evaluate the rheological response under elongational flow. It has been recognized that drawdown force has information on uniaxial elongational viscosity.^{39,40} Furthermore, the method is available for various polymers, including a polymer having low viscosity. In this study, the measurements were performed at

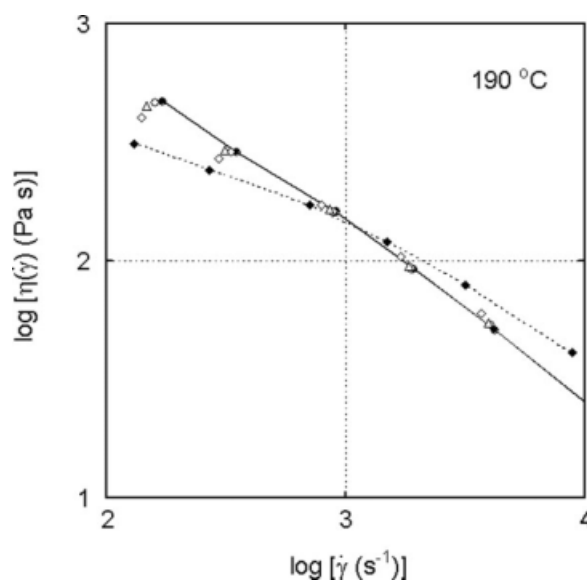


Figure 7 Steady-state shear viscosity measured by a capillary rheometer at 190°C for PP (closed circles with a solid line), PP/LLDPE (80/20) (open triangles), PP/LLDPE (50/50) (open diamonds), and LLDPE (closed diamonds and a dotted line).

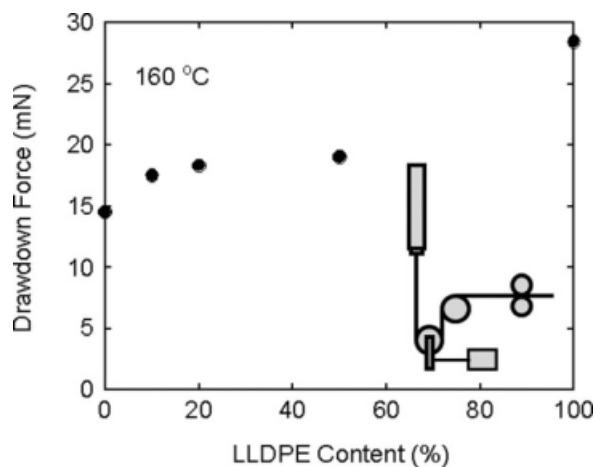


Figure 8 Drawdown force for the samples at 160°C. The measurement method is illustrated in the figure.

low temperature (160°C), because the level of the drawdown force is significantly low, especially at the processing temperature. It is found from Figure 8 that drawdown force increases with LLDPE content, although the shear viscosity of LLDPE is significantly lower than that of PP. The result suggests that the LLDPE employed exhibits a marked strain-hardening behavior in elongational viscosity. This could be attributed to the low-density polyethylene

in LLDPE. Furthermore, the drawdown force of the blends, which corresponds with strain-hardening in uniaxial elongational viscosity,³⁹ increases with LLDPE content. These experimental results indicate good processability at extrusion coating, because neck-in level is mainly determined by the degree of strain-hardening in elongational viscosity.^{8,40-43}

Processability

The head pressure, which is defined as the pressure at the end of the screw, and the motor torque were monitored during the extrusion test. As is well known, the head pressure is drastically affected by the shear viscosity in a molten state, which is successfully predicted by Tadmor and Klein.⁴⁴ In this study, the order of the head pressure, shown in [Fig. 9(a)] corresponds with the shear viscosity shown in Figure 6. Although the shear viscosities in Figures 6 and 7 are measured at 190°C, the order at extrusion temperature (260°C), would not change because both PP and LLDPE show a similar level of flow activation energy, as explained. In contrast to the head pressure, PP shows the highest motor torque [Fig. 9(b)]. Although the exact mechanism of the high torque is unknown, it could be attributed to the narrow size distribution of PP pellets (the data is not

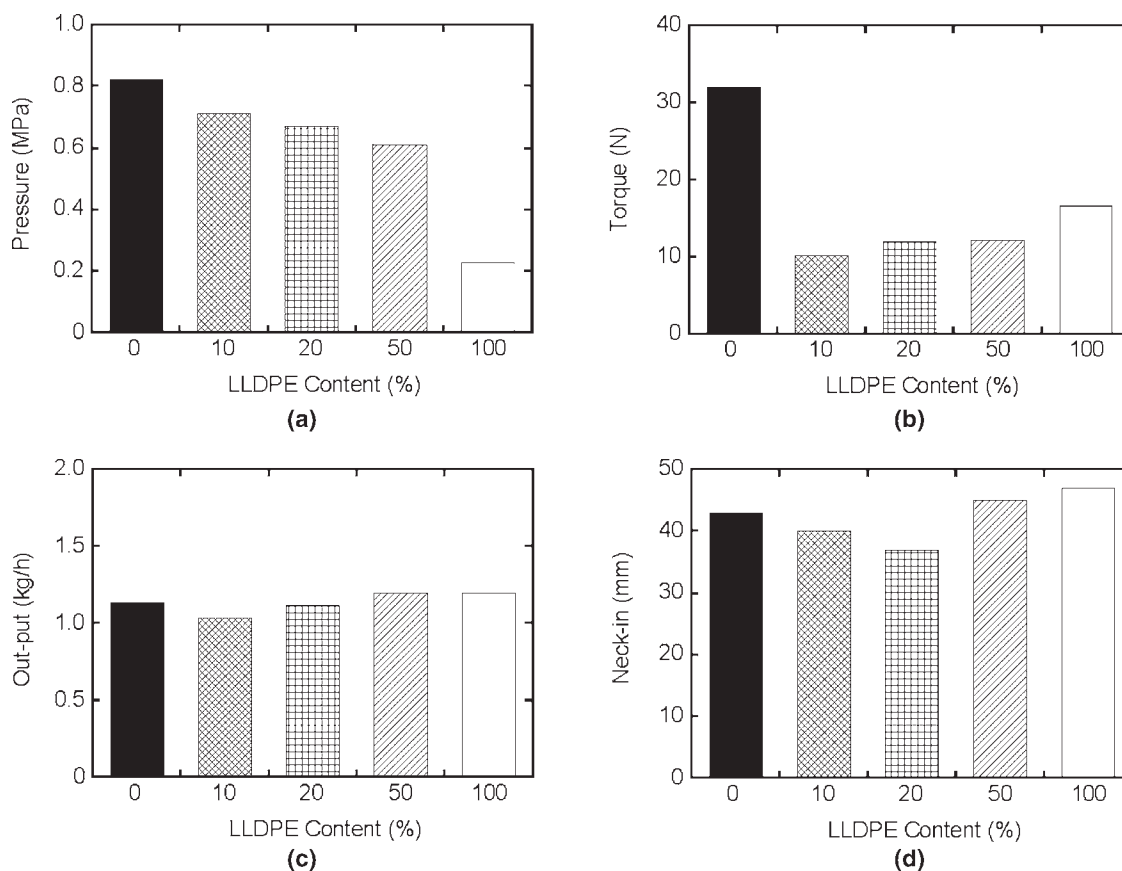


Figure 9 Various processing parameters: (a) pressure, (b) torque, (c) out-put, and (d) neck-in level.

presented here). As the extruder employed is a laboratory scale, pellet size has a great influence on the solid conveying.⁴⁵ Thus, lack of large size pellets accelerates the solid conveying, leading to a high degree of volume filling. Moreover, it is found that blending a small amount of LLDPE decreases the motor torque significantly, indicating that bulk density of the pellets decreases by mixing LLDPE pellets. The order of the output rate could be explained by the same reason [Fig. 9(c)].

Furthermore, the neck-in level was also evaluated following the illustration in Figure 1. As shown in Figure 9(d), the neck-in level of PP/LLDPE (80/20) is considerably lower than that of PP, owing to strain-hardening behavior in elongational viscosity. However, LLDPE and PP/LLDPE (50/50) show large neck-in. Although the exact mechanism is unknown, low shear viscosity could be responsible for the phenomenon.

Mechanical properties

Figure 10 shows the oscillatory tensile moduli, such as storage modulus E' and loss modulus E'' , as a function of temperature. Beyond the glass transition temperature (T_g) of PP, which is located approximately at 0°C, E' of the blends decreases moderately and falls off sharply around 100°C. The figure also shows that heat resistance nature is suppressed with increasing LLDPE content. Moreover, apparent double peaks are detected in the E'' curve in the temperature range between -60 and 50°C for PP/LLDPE (50/50). The peak located at high temperature is ascribed to T_g of PP and that at low temperature is to T_g of LLDPE. The result shows that the blend system shows apparent phase-separated structure.

The yield stress and tensile strength at break are shown in Figure 11. The experimental error of both properties was within 5%. The yield stress of the MD sample is apparently higher than that of the TD, irrespective of the blend ratio, suggesting that the films exhibit molecular orientation. Furthermore, the yield stress of PP/LLDPE (50/50) is fairly lower than those of PP and the other blends. Considering that LLDPE shows lower shear viscosity than PP, the continuous phase of PP/LLDPE (50/50) could be LLDPE. This is the reason for the low yield stress.

Figure 11(b) shows that the ultimate tensile strength in MD is lower than that in TD for PP. In contrast, LLDPE shows higher strength in MD. Furthermore, the tensile strength in TD of the blends decreases with increasing blend ratio of LLDPE. However, in the machine direction, PP/LLDPE (80/20) gives the highest tensile strength. As a result, MD/TD balance varies with the blend ratio. The minimum MD/TD balance, that is, weak or no mechanical anisotropy, is achieved by blending 20% of

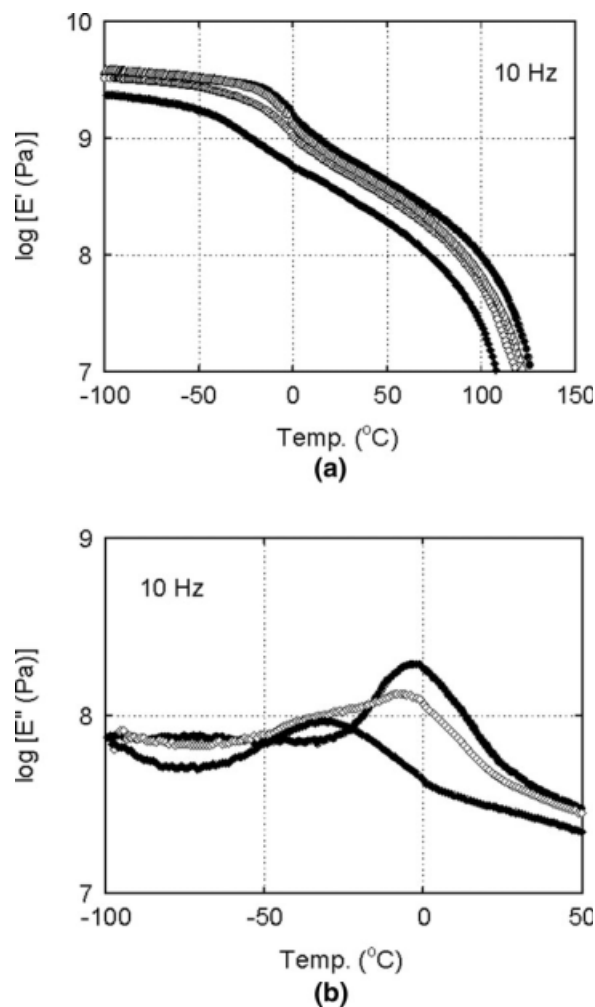


Figure 10 Temperature dependence of (a) tensile storage modulus E' and (b) loss modulus E'' at 10 Hz for PP (closed circles), PP/LLDPE (80/20) (open triangles), PP/LLDPE (50/50) (open diamonds), and LLDPE (closed diamonds).

LLDPE. Currently, the origin of the anomalous mechanical anisotropy has not been clarified. Orientation of crystalline aggregates of PP and the distribution and shape of LLDPE particles could lead to the complicated mechanical response.

CONCLUSION

Rheological properties, thermal properties, processability at extrusion coating, and mechanical properties are studied for blends composed of PP and LLDPE produced by metallocene catalyst. The characterization of the individual polymers clarified that the LLDPE employed is composed of two or more components of polyethylene. The major fraction is an LLDPE produced by metallocene catalyst. Furthermore, a low-density PE is also blended. Although the blends show phase-separated morphology, which is suggested by oscillatory shear

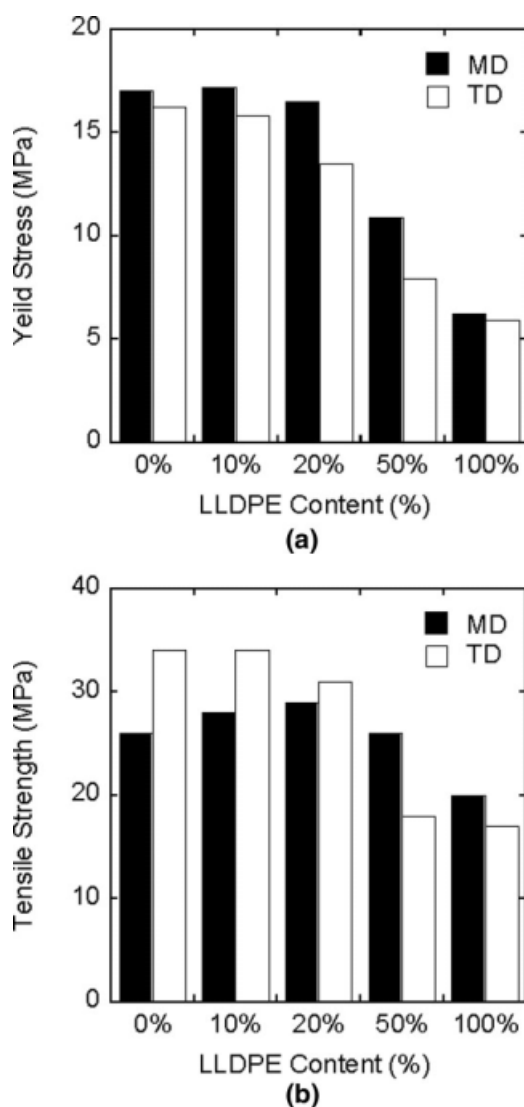


Figure 11 Tensile properties of the extruded films: (a) yield stress and (b) ultimate stress at break.

modulus, the drawdown force increases with LLDPE content. This should be noted because the shear viscosity of the LLDPE is significantly lower than that of PP. The enhanced drawdown force is responsible for the low level of neck-in. Moreover, the blend with 20% of LLDPE shows lower motor torque and head pressure than pure PP. Finally, the anisotropy of ultimate tensile strength is reduced for the blend with 20 wt % of LLDPE.

References

1. Bezigian, T. *Extrusion Coating Manual*, 4th ed.; TAPPI Press: Atlanta, 1998.
2. White, J. L.; Choi, D. D. *Polyolefins*; Hanser: Munich, 2004.
3. Larson, R. G. *J Rheol* 1984, 28, 545.
4. Wagner, M. H.; Schaeffer, J. *J Rheol* 1992, 36, 1.
5. McLeish, T. C. B.; Larson, R. G. *J Rheol* 1998, 42, 81.
6. Wagner, M. H.; Yamaguchi, M.; Takahashi, M. *J Rheol* 2003, 47, 779.
7. Yamaguchi, M. In *Polymeric Foams: Mechanisms and Materials*; Lee, S. T.; Ramesh, N. S., Eds.; CRC Press: Boca Raton, 2004; p 19.
8. Campbell, G. A.; Sweeney, P. A. In *Film Processing*; Kanai, T.; Campbell, G. A., Eds.; Hanser: Munich, 1999; p 141.
9. Junk, H. W.; Hyun, J. C. In *Polymer Processing Instability*; Hatzikiriakos, S. G.; Migler, K. B., Eds.; Marcel Dekker: New York, 2005; p 321.
10. Pasquini, N. *Polypropylene Handbook*, 2nd ed.; Hanser: Munich, 2005.
11. Higgmann, R.; Marczinke, B. L. *J Rheol* 1994, 38, 573.
12. Lagendijk, R. P.; Hogt, A. H.; Buijtenhuijs, A.; Gotsis, A. D. *Polymer* 2001, 42, 40035.
13. Auhl, D.; Stange, J.; Münstedt, H.; Krause, B.; Voigt, D.; Lederer, A.; Lappan, U.; Lunkwitz, K. *Macromolecules* 2004, 37, 9465.
14. Graebing, D. *Macromolecules* 2005, 38, 4602.
15. Yamaguchi, M.; Wagner, M. H. *Polymer* 2006, 47, 3629.
16. Yamaguchi, M.; Miyata, H. *Polym J* 2000, 32, 164.
17. Andersson, T.; Wesslén, B.; Sandström, J. *J Appl Polym Sci* 2002, 86, 1580.
18. Utracki, L. A. *Polymer Alloys and Blends: Thermodynamics and Rheology*; Hanser: Munich, 1989.
19. Lohse, D. J.; Graessley, W. W. In *Polymer Blends*; Paul, D. R.; Bucknall, C. B., Eds.; Wiley: New York, 1999; p 219.
20. Nitta, K.; Yamaguchi, M. In *Polyolefin Blends*; Nwabunma, D.; Kyu, T., Eds.; Wiley: New York, 2008; p 224.
21. Yamaguchi, M.; Miyata, H.; Nitta, K. *J Appl Polym Sci* 1996, 62, 87.
22. Yamaguchi, M.; Miyata, H. *Macromolecules* 1999, 32, 5911.
23. McNally, T.; McShane, P.; Nally, G. M.; Murphy, W. R.; Cook, M.; Miller, A. *Polymer* 2002, 43, 3785.
24. Carriere, C. J.; Silvis, H. C. *J Appl Polym Sci* 1997, 66, 1175.
25. Razavi-Nouri, M. *Polym Test* 2007, 26, 108.
26. Chaffin, K. A.; Knutsen, J. S.; Brant, P.; Bates, F. S. *Science* 2000, 288, 2187.
27. Isasi, J. R.; Haigh, J. A.; Graham, J. T.; Mandelkern, L.; Alamo, R. G. *Polymer* 2000, 41, 8813.
28. Yamaguchi, M.; Abe, S. *J Appl Polym Sci* 1999, 74, 3153.
29. Mäder, D.; Heinemann, J.; Walter, P.; Mülhaupt, R. *Macromolecules* 2000, 33, 1254.
30. Sehanobish, K.; Patel, R. M.; Croft, B. A.; Chum, S. P.; Kao, C. A. *J Appl Polym Sci* 1994, 51, 887.
31. Hong, H.; Zhang, Z.; Chung, T. C. M.; Lee, R. W. *J Polym Sci Part B: Polym Phys* 2007, 45, 639.
32. Keating, M. Y.; Lee, I. *J Macromol Sci Phys* 1999, 38, 379.
33. Ferry, J. D. *Viscoelastic Properties of Polymers*, 3rd ed.; Wiley: New York, 1980.
34. Vega, J. F.; Santamaria, A.; Munoz-Escalona, A.; Lafuente, P. *Macromolecules* 1998, 31, 3639.
35. Van Gurp, M.; Palmen, J. *Rheol Bull* 1998, 67, 5.
36. Wagner, M. H.; Kheirandish, S.; Yamaguchi, M. *Rheol Acta* 2004, 44, 198.
37. Palierne, J. F. *Rheol Acta* 1990, 29, 204.
38. Graebing, D.; Müller, R.; Palierne, J. F. *Macromolecules* 1993, 26, 320.
39. Bernnat, A. Ph.D. Thesis, University of Stuttgart, Stuttgart, 2001.
40. Yamaguchi, M.; Takahashi, M. *Polymer* 2001, 42, 8663.
41. Debroth, T.; Erwin, L. *Polym Eng Sci* 1986, 26, 462.
42. Debroth, T.; Erwin, L. *ANTEC* 1986, 893.
43. Kouda, S. *Polym Eng Sci* 2008, 48, 1094.
44. Tadmor, Z.; Klein, I. *Engineering Principles of Plasticating Extrusion*; Van Nostrand Reinhold: New York, 1970.
45. Rauweendaal, C.; Noriega, M. P. *Troubleshooting the Extrusion Process*; Hanser: Munich, 2001.